

Electronic structure of holmium

R. I. R. Blyth

Surface Science Research Centre, University of Liverpool, Liverpool L69 3BX, United Kingdom

S. D. Barrett

*Surface Science Research Centre, University of Liverpool, Liverpool L69 3BX, United Kingdom
and Department of Physics, Oliver Lodge Laboratory, University of Liverpool, Liverpool L69 3BX, United Kingdom*

S. S. Dhesi, R. Cosso, and N. Heritage

Surface Science Research Centre, University of Liverpool, Liverpool L69 3BX, United Kingdom

A. M. Begley and R. G. Jordan

Alloy Research Center, Department of Physics, Florida Atlantic University, Boca Raton, Florida 33431-0991

(Received 18 April 1991)

We report a study of the valence-band electronic structure of the rare-earth metal holmium. Angle-resolved ultraviolet photoemission experiments have been performed on Ho(0001) and the results compared to first-principles photocurrent calculations. The photoemission results show a number of well-resolved features that do not disperse with photon energy for $h\nu > 20$ eV. We identify one of these features, at a binding energy of 1.7 eV, as emission from the Γ_{4-} point of the bulk band structure. Considerable dispersion of some of these features with emission angle has enabled us to map, in detail, the experimental bands of the (0001) surface along the ΓM and ΓKM symmetry directions. Comparison of the experimental spectra with photocurrent calculations employing a realistic potential in the surface layers suggests that the remaining features are due to surface effects. The binding energy of one of the calculated peaks is higher by 0.9 ± 0.05 eV than that seen in experiment and possible reasons for this discrepancy are discussed.

I. INTRODUCTION

The valence electronic configuration of all the hexagonal-close-packed (hcp) rare-earth metals is of the form $[nd(n+1)s]^3$ where $n=3$ (Sc), 4 (Y), or 5 (La and the lanthanides), which accounts for their similar chemical properties. In addition, the lanthanides also have a varying number of highly localized $4f$ levels, some of which may be energetically degenerate with the valence band. This degeneracy leads to many interesting mixed-valence phenomena in lanthanide compounds.¹ Rare earths are also being increasingly investigated in metal-semiconductor contacts² because of the low Schottky barrier heights of the resulting interfaces. The valence electronic structure of rare-earth metals is thus an area of considerable scientific and technological interest, and we have investigated the hcp lanthanide metal holmium with angle-resolved uv photoemission spectroscopy (ARUPS) of the (0001) surface, using synchrotron radiation. It would have been beneficial to perform experiments on the other principal faces of Ho, but we have shown recently³ that both these surfaces undergo a reconstruction to a structure almost identical to the (0001) surface. Thus we are unable to obtain additional information on the electronic structure from studies of these surfaces.

There have been a large number of band-structure calculations performed for the hcp rare-earth metals,⁴ and although no calculations for Ho have appeared in the literature the similarity between the band structures of

these closely related metals means that this does not represent a serious omission. However, most of these were not self-consistent and many were nonrelativistic which, given the high atomic numbers of the lanthanides, would tend to lessen their effectiveness. We have therefore calculated self-consistently the relativistic band structure of Ho.

ARUPS is now well established as the preferred method of investigating the valence electronic structure of solids⁵ since it is able to measure simultaneously both the energy and at least two components of the momentum of the photoemitted electrons. Because of the low energy of these electrons their mean free path (mfp) is very short—of the order of a few atomic layers—and the resulting surface sensitivity means that it is essential to prepare and maintain clean, well-ordered single-crystal surfaces of the material to be studied. In the case of the rare-earth metals this presents substantial difficulties. Firstly, growth of high-purity single crystals of sufficient size to perform ARUPS measurements is considerably more troublesome than is the case for transition metals.⁶ Fortunately, work done at Ames Laboratory, Iowa State University, U.S.A., and the School of Metallurgy and Materials, University of Birmingham, United Kingdom, is easing this problem—all the ARUPS studies of rare-earth metals reported in the literature to date have used samples obtained from one of these two sources. Secondly, their high reactivity ensures that sample cleaning is a particularly difficult task. Because of these factors there

have been relatively few ARUPS studies of rare-earth metals. The first of these, of Gd(0001),⁷ showed apparently good agreement with a non-spin-polarized band-structure calculation.⁸ However, a more recent spin-polarized calculation⁹ shows much worse agreement. Gd is ferromagnetic with a Curie point close to room temperature (and a surface Curie point 22 K higher¹⁰) and so until spin-polarized ARUPS experiments are performed on Gd it is difficult to be sure of the magnetic effects on the photoemission spectra. This problem was not encountered by Wu *et al.* in their study of Tb(0001) (Ref. 11) as Tb is paramagnetic at temperatures above 217 K (Ref. 4) but, unlike Gd, part of the valence band is obscured by 4*f* emission. In addition they experienced severe difficulties with Fe contamination, with ~15% of a monolayer present on their “clean” surface. Two different crystallographic surfaces of Y have been studied by Barrett and co-workers,^{12–14} the (1120) surface showing a reconstruction^{13,14} similar to that observed on the same surfaces of Ho and Er.³ Only one of the peaks seen on Y(0001) (Ref. 12) seemed to be explicable in terms of one-electron bulk bands, with many-body effects apparently predominating. There have also been two ARUPS studies of Ce(001),^{15,16} but since the properties of this cubic metal differ markedly from those of the hcp rare earths their results are not relevant to this work. Ho is particularly suited to ARUPS experiments as the 4*f* peaks, which occur in the binding energy range 4.5–10.5 eV,¹⁷ do not obscure any part of the valence band, unlike Tb, and is nonmagnetic at room temperature, unlike Gd. It is also a “typical” lanthanide in that it has a partially filled *f* shell and the hcp crystal structure. Thus photoemission results from Ho should be generally applicable to the rest of the series.

Direct comparison of ARUPS data with band-structure calculations presents three difficulties. (1) The calculations are generally performed assuming an infinite lattice, whereas the short mfp of electrons in solids limits the photoemission probe to the surface region, (2) some form of empirical expression for the final state is generally used in order to determine k_{\perp} , the component of electron momentum perpendicular to the surface. This introduces arbitrary parameters, such as the “inner potential” required if the free-electron final-state approximation is used, and it is often unclear how valid these empirical expressions are. (3) Many-body effects in the photoemission process may introduce satellites or peak shifts which will not be reproduced in one-electron calculations. To avoid the first two of these problems we have compared our ARUPS data with *ab initio* photocurrent calculations, in which the final state is explicitly calculated, using potentials generated by a slab calculation to model the effects on the electronic structure produced by the presence of the surface. These calculations further improve on direct comparison by including momentum and lifetime broadenings.

II. BAND-STRUCTURE CALCULATIONS

Self-consistent band-structure calculations, within the local density approximation, were performed on the Convex C-220 at the Science and Engineering Research

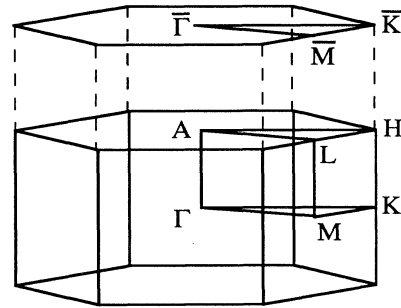


FIG. 1. The Brillouin zones of the bulk hcp lattice and the (0001) surface.

Council (SERC) Daresbury Laboratory, United Kingdom. The linear muffin-tin orbital (LMTO) method¹⁸ with the atomic sphere approximation (ASA) were used. The ASA replaces the Wigner-Seitz polyhedra of the solid by overlapping Wigner-Seitz spheres, an approximation particularly suited to close-packed elemental solids. The experimentally observed lattice parameters⁶ were used, and 225 *k* points sampled in the irreducible wedge of the Brillouin zone (Fig. 1). The von Barth–Hedin¹⁹ form for the local exchange and correlation was employed and calculations performed for a scalar relativistic Hamiltonian (i.e., including mass-velocity and Darwin terms) with spin-orbit coupling introduced variationally.²⁰ The highly localized 4*f* levels were treated as part of the core, with their occupancy fixed at 10, i.e., that observed in solid Ho,²¹ giving an outer electronic configuration of (5*d* 6*s*)³, the core eigenvalues being determined by an atomic scheme. Spin polarization was not included. The energy bands and angular-momentum-resolved densities of states (DOS) produced by this calculation are shown in Fig. 2. The bands are very similar to the fully relativistic LMTO bands of Tb calculated by Wu *et al.*,¹¹ which is to be expected as Tb has the same outer electronic configuration and (hcp) crystal structure. The principal difference is that in Ho a band crosses the *M* point just below the Fermi level, whereas in Tb it does so just above. The Ho bands and DOS are also very similar to those of Y,^{22,23} reinforcing the idea that Y can be considered a “prototype” rare earth, i.e., one without *f* electrons but with an otherwise similar electronic structure. The main difference is that the occupied bandwidth of Y is somewhat narrower; the Y Γ_{1+} point is at 4.9 eV below the Fermi level^{22,23} compared to 5.5 eV in Ho. Since we compare our ARUPS data with nonrelativistic photocurrent calculations, a nonrelativistic band-structure calculation was performed in order to determine the differences between the relativistic and nonrelativistic bands. The bands and DOS produced by this calculation are shown in Fig. 3. As might be expected several band crossings now become allowed; notably, just below the Fermi level close to the *K* point, and at the *M* point 2 eV below the Fermi level. The Γ_{1+} point now occurs 0.95 eV higher in energy, as the lack of relativistic effects reduces the occupied bandwidth.

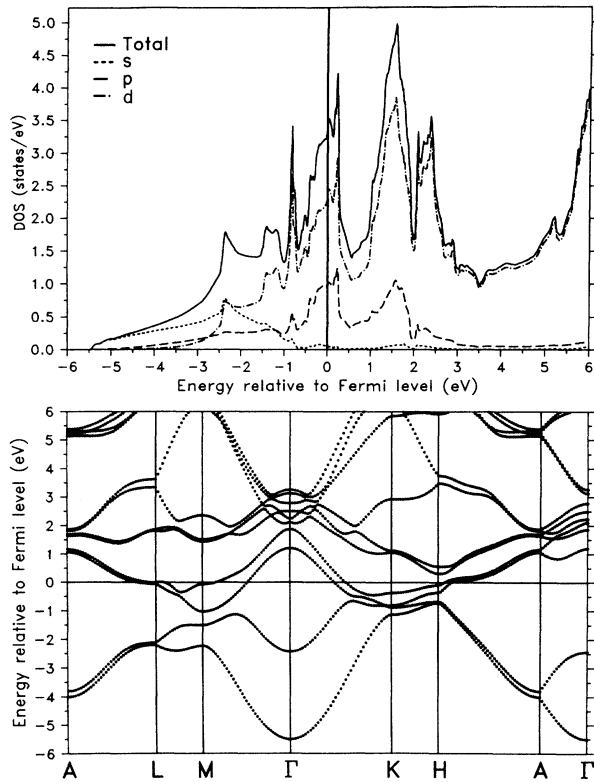


FIG. 2. Relativistic energy bands and densities of states for hcp Ho, with the $4f$ electrons treated as part of the core.

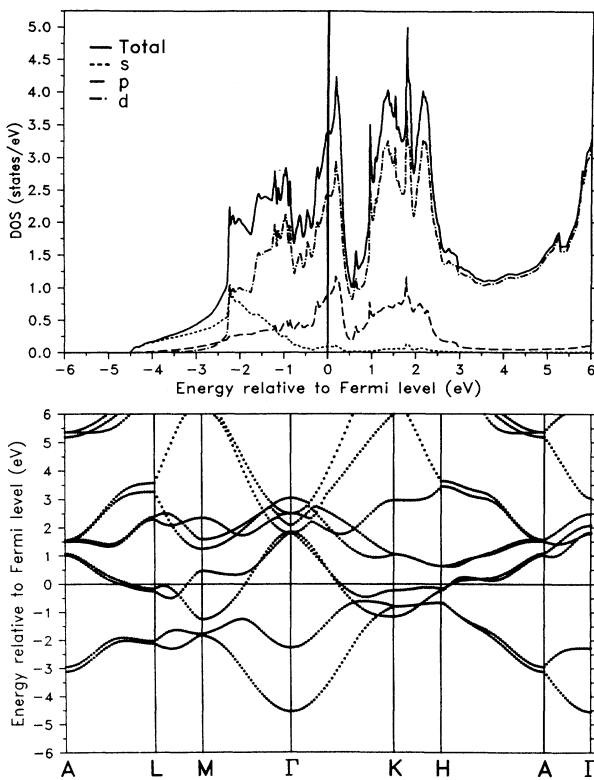


FIG. 3. Nonrelativistic energy bands and densities of states for hcp Ho, with the $4f$ electrons treated as part of the core.

III. ARUPS EXPERIMENTS

The Ho(0001) sample was cut from the same high-quality single-crystal boule as the (11 $\bar{2}$ 0) sample used in our study of the surface reconstruction.³ The boule, grown by Dr. D. Fort (School of Metallurgy and Materials, University of Birmingham, U.K.), had an impurity concentration of ~ 0.1 at. %, with C and O the dominant impurities. The sample was spark machined from the boule and polished *ex situ* using standard metallographic techniques.

The photoemission experiments were performed using the toroidal grating monochromator (TGM) on beamline 6.2 of the Synchrotron Radiation Source (SRS), SERC Daresbury Laboratory, United Kingdom. The spectrometer used was a Vacuum Generators ADES 400 system with three-grid low-energy electron diffraction (LEED) optics used as a retarding field analyzer for Auger electron spectroscopy (AES). The overall energy resolution for ARUPS was 0.15 eV. The base pressure of the system during the ARUPS experiments was $\sim 2 \times 10^{-10}$ mbar, with the main residual gases being Ar, H₂, and CO.

In situ sample cleaning was performed by repeated cycles of Ar⁺ bombardment (beam energy 3–4 kV, current density $\sim 20 \mu\text{A}/\text{cm}^2$) and annealing at 875 K. Surface cleanliness and order were monitored principally by ARUPS—contamination shows as additional weight in the spectra at ~ 6 eV binding energy and the intensity of the surface-order-dependent state (SODS) at 9.6 eV binding energy is known to be extremely sensitive to the quality of the surface.^{3,12,13,24} Spectra of Ho(0001) in the binding energy range 0–12 eV, including the SODS, are shown and discussed elsewhere.^{3,24} After ~ 20 cleaning cycles a high SODS intensity and low contamination level were reproducibly obtainable, the cleanliness and crystallinity being confirmed by AES (C and O levels of a few at. %) and LEED (sharp 1×1 spots on a relatively low background).

Normal-emission valence-band ARUPS spectra for a range of photon energies, corresponding to emission from states along the ΓA direction of the Brillouin zone, are shown in Fig. 4. There are four features, none of which show any significant dispersion with photon energy: three peaks labeled *a*, *b*, and *c*, at binding energies of 0.3, 1.7, and 2.9 eV, respectively, and a shoulder at ~ 4 eV. The same features have been seen on Gd(0001) (Refs. 7 and 25) and Y(0001),¹² with the exception that the 4-eV shoulder is not seen on Y(0001).¹² The Gd(0001) spectra⁷ were taken over a different photon energy range and so the dependence of peak intensity upon photon energy cannot be directly compared. For Y(0001) (Ref. 12) the photon energy dependence is extremely similar to Ho; peaks *a*, *b*, and *c* resonate at $h\nu = 38, 30,$ and 40 eV respectively, compared to $40, 28,$ and 40 eV for Ho(0001). This represents strong experimental evidence that the band structures of Ho and Y are indeed very similar, as was suggested in Sec. II. In both cases peaks *a* and *c* resonate at very similar energies, which suggests that they may share a common origin, while the significantly different photon energy dependence of peak *b* suggests a

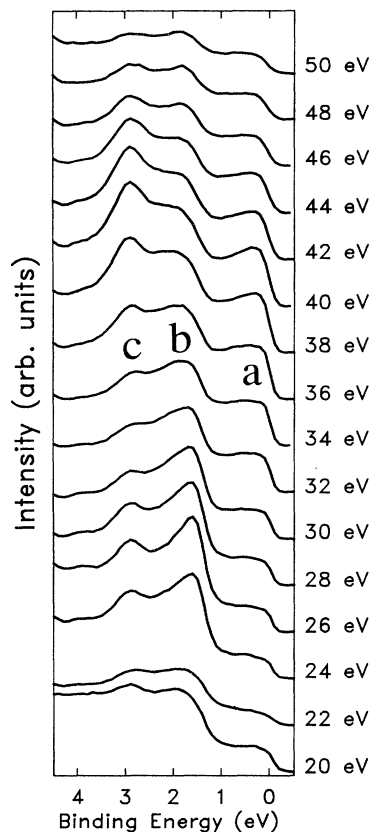


FIG. 4. Flux-normalized normal-emission ARUPS spectra of Ho(0001), taken using p -polarized synchrotron radiation, photon incidence angle of 30° .

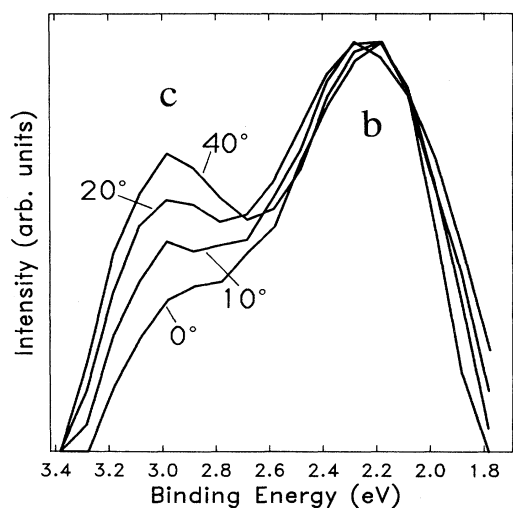


FIG. 5. ARUPS spectra of Ho(0001) for different photon incidence angles (relative to surface normal); emission angle of 30° , photon energy of 40 eV, p -polarized radiation. The spectra have been normalized to the intensity of peak b .

different origin for this peak. Dispersion of valence-band features with photon energy has been seen on Gd(0001) (Ref. 7) and Tb(0001),¹¹ but in both cases this occurred for $h\nu < 20$ eV. Himpsel and Reihl⁷ suggested that the lack of dispersion at higher photon energies was due to the exceptionally short mfp of electrons in rare-earth metals, resulting in considerable k_{\parallel} broadening. Thus the spectra are dominated by regions of high DOS. At lower photon energies the kinetic energies of the photoemitted electrons are lower, the mfp increases, and the broadening is reduced sufficiently for dispersion to be observable. Unfortunately, due to the design of the monochromator, we were unable to take spectra for $h\nu < 20$ eV without considerable interference from second-order light. Barrett and Jordan¹² found that the behavior of peak b on Y(0001) was well reproduced by photocurrent calculations which utilized bulk Y potentials, and concluded that this peak was due to emission from the Γ_{4-} point of the bulk Y band structure. Given the close similarity between the behavior of peak b on Y(0001) (Ref. 12) and Ho(0001), and between the calculated band structures of Y (Ref. 20) and Ho we conclude the peak b on Ho(0001) is due to emission from the Γ_{4-} point of the Ho band structure. Barrett and Jordan¹² were unable to fully account for peaks a or c on Y(0001)—they were not reproduced in their photocurrent calculations, although a peak at the Fermi level could be produced by truncation and convolution²³—and suggested that peak a may have been due to a surface state and peak c to a many-body effect. Himpsel and Reihl⁷ suggested that peaks b and c (to use our notation) in their Gd(0001) spectra were due to emission from, respectively, the Γ_{4-} and Γ_{1+} points of the same Δ_1 band in the Gd band structure. However, these peaks on Ho(0001) exhibit different polarization dependence (Fig. 5), and must therefore originate from initial-state bands of different symmetry. Thus, if we assume peaks b and c share the same origins on Gd(0001) as on Ho(0001), and that peak b on Gd(0001) is due to emission from the Gd Γ_{4-} point, it follows that Himpsel and Reihl⁷ incorrectly assigned peak c to emission from the Gd Γ_{1+} point. The Tb(0001) spectra of Wu *et al.*¹¹ bear little resemblance to those of Gd(0001),⁷ Y(0001),¹² or Ho(0001). This is surprising given the similarity between their Tb band-structure calculation and those of Y (Refs. 20 and 21) and Ho, and suggests that the effects of the Fe contamination of their sample may have been somewhat greater than they acknowledge. Since they observe the Tb Γ_{4-} point at 3.6 eV binding energy, more than 1 eV greater than the values found for Gd,⁷ Y,¹² or Ho, it follows that the apparent shift of the Tb Δ_1 band to a binding energy 1.5 eV greater than the calculated position, which they conclude as being characteristic of the clean Tb surface, may well be an artifact of the Fe contamination.

Off-normal-emission spectra of Ho(0001), with the emission angles chosen such that k_{\parallel} , the component of electron momentum parallel to the surface, varies along the two high symmetry directions of the surface Brillouin zone (see Fig. 1), $\Gamma K M$ and ΓM , are shown in Fig. 6. Plots of binding energy against k_{\parallel} are shown in Fig. 7, with k_{\parallel} , determined using the well-known expression

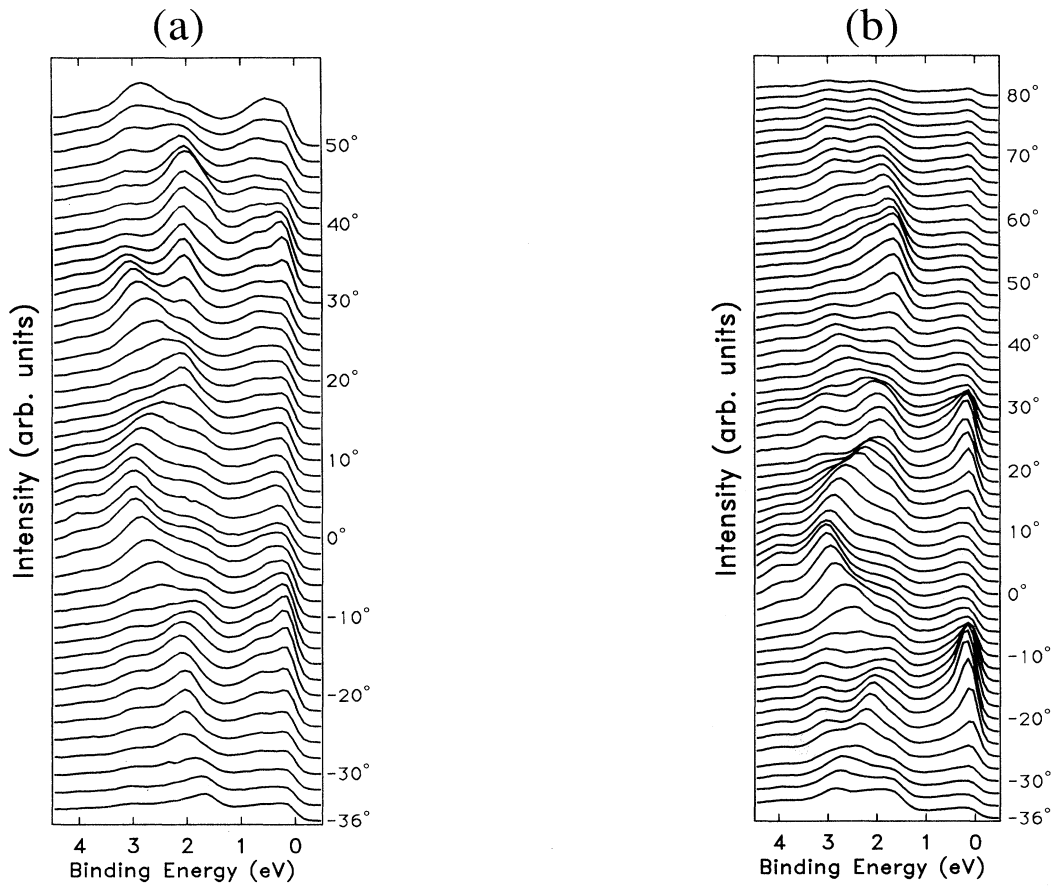


FIG. 6. Flux-normalized off-normal-emission ARUPS spectra of Ho(0001), with emission angles chosen to vary k_{\parallel} along (a) ΓKM and (b) ΓM . Photon energy is 40 eV, p -polarized radiation incident at 55°.

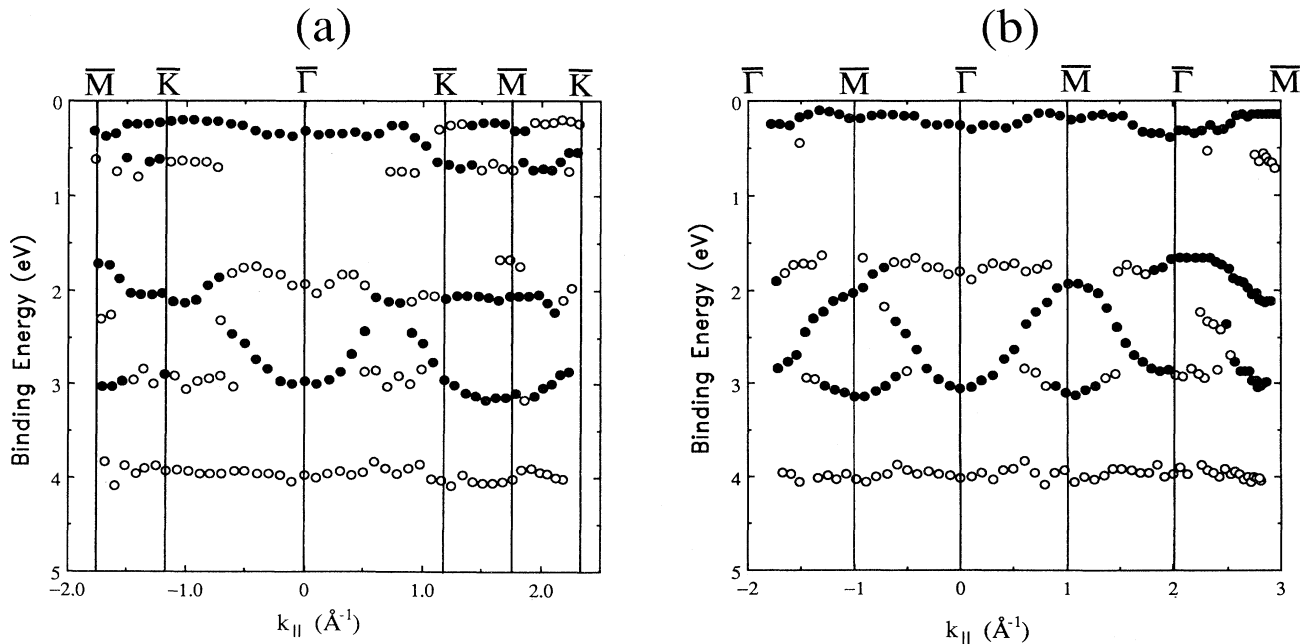


FIG. 7. Graphs of binding energy vs k_{\parallel} , determined from the data of (a) Fig. 6(a) and (b) Fig. 6(b). The solid circles correspond to peaks, and the open circles to shoulders.

$$k_{\parallel} = (2m_e/\hbar^2)^{1/2}(E_{\text{kin}})^{1/2}\sin\theta, \quad (1)$$

where m_e is the electron rest mass, \hbar is Planck's constant divided by 2π , E_{kin} is the electron kinetic energy, and θ is the emission angle relative to surface normal. There is obviously considerable dispersion evident in these spectra, in marked contrast to the normal-emission data. There are several other points of note. (i) The intensity at the Fermi level is considerably enhanced at the first M points [corresponding approximately to $\theta = \pm 20^\circ$ in Fig. 6(b)], yet not at the K points, in agreement with the data of Himpsel and Reihl⁷ on Gd(0001). This is opposite to what would be expected from the band structure (Fig. 2) as there is a close grouping of four bands along KH close to the Fermi level, and only two along LM . (ii) There is a gap between ~ 0.5 and ~ 1.5 eV binding energy which is not present in the band structure (Fig. 2). Momentum broadening may well be responsible for this apparent discrepancy; off-normal-emission photocurrent calculations for Y(0001) (Ref. 21) show that peak b , which is due to emission from the bulk band structure, exhibits negligible dispersion with emission angle. Thus instead of observing the dispersion of the bulk band we see emission from the Γ_{4-} point, where the DOS is high, and the dispersion of peak c , which is *not* due to emission from bulk one-electron bands. (iii) A band appears to cross the Fermi level between Γ and K , and possibly also between Γ and M , although in the latter case this is difficult to determine owing to the enhanced emission at the Fermi level close to M . These may well correspond to the crossings seen along ΓK and ΓM in the band structure, but *direct* comparison of the crossing points and dispersions seen in Fig. 7 with the calculated band structure is not possible, as k_{\perp} is unknown. Indirect comparison may be made by comparing the spectra with *ab initio* photocurrent calculations, which are instructive in identifying the features in the normal-emission spectra which do not appear to be derived from bulk one-electron bands, i.e., peaks a and c .

IV. PHOTOCURRENT CALCULATIONS

Photocurrent calculations were performed using the (nonrelativistic) NEWPOOL code²⁶ on the Cray XMP/48 at SERC Rutherford Appleton Laboratory, United Kingdom. In the NEWPOOL scheme the angle-resolved photocurrent is calculated for a semi-infinite array of nonoverlapping muffin-tin potentials (Fig. 8), with the surface modeled by a step potential in contact with the outermost layer of muffin tins. In an attempt to model the surface more realistically we used the potentials generated by a supercell slab calculation, performed on the Floating Point Systems FPS-264 processor at Daresbury Laboratory. A self-consistent LMTO-ASA calculation was performed, treating the f levels as part of the core. The unit cell consisted of five layers of Ho and five layers of vacuum (empty spheres) in an $ABAB$ stacking sequence (Fig. 9). The resulting potentials from layers 1, 2, and 3 were placed on layers a , b , and c , respectively, of the NEWPOOL array. With the exception of Sc(0001) (Ref. 27) there

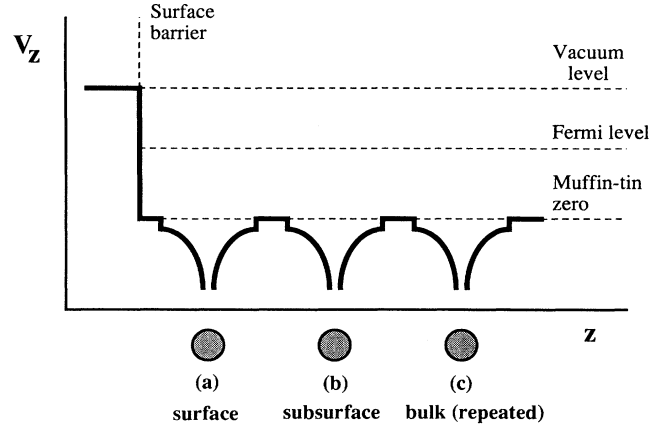


FIG. 8. The model of the surface potential used in the NEWPOOL code.

have been no quantitative LEED studies of rare-earth metals and thus there is no information as to the surface layer spacing: the bulk layer spacing was therefore used. The NEWPOOL code using LMTO slab potentials has been employed recently by Jordan *et al.*²⁸ to model the photoemission from the $4p$ levels of Y(0001), obtaining excellent agreement with the experimental line shapes. Thus we believe the use of slab potentials considerably improves the surface modeling.

A normal-emission photocurrent calculation for the valence band of Ho(0001) is shown in Fig. 10. Note that, in contrast to the Y(0001) calculations of Barrett and Jordan,¹² the existence of peak a is reproduced, as is that of the 4-eV shoulder. The calculated peak a probably arises from the truncation of the tail of an unoccupied surface

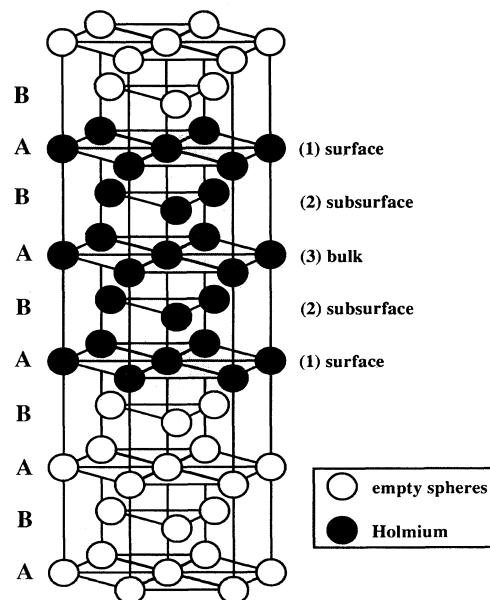


FIG. 9. The unit cell used in the LMTO "supercell" slab calculation.

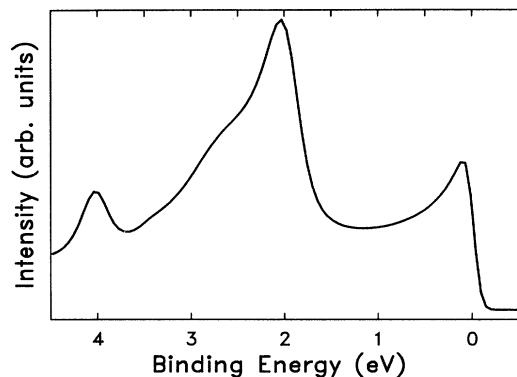


FIG. 10. Calculated normal-emission spectrum, photon energy 40 eV, p -polarized radiation incident at 30° . The calculated photocurrent has been truncated at the Fermi level and convoluted with a Gaussian of full width at half maximum equal to 0.15 eV to simulate the experimental resolution.

state. It does not show the same photon energy dependence as the experimental peak a , but the polarization dependence is reproduced correctly. The intensity of the experimental peak a was gradually attenuated with time as the sample contamination level increased, and could be greatly reduced by a very light Ar^+ bombardment (500

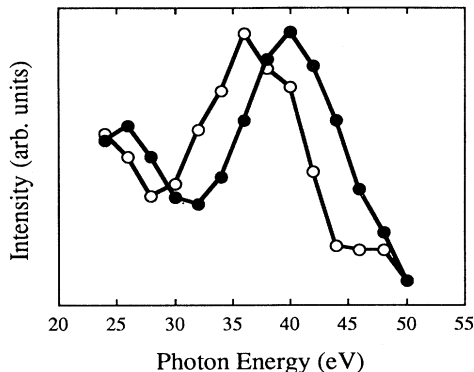


FIG. 11. The (flux-normalized) intensity variation of peak c (solid circles) and that of the calculated peak at 2.05 eV binding energy (open circles).

eV for $\sim 15\text{s}$) as has also been reported for peak a on $\text{Y}(0001)$ (Ref. 12). This suggests the involvement of a surface state and there is evidence for such an (unoccupied) state from inverse photoemission results on $\text{Y}(0001)$.^{24,29}

It appears from Fig. 10 that peak b is reproduced, at 2.05 eV binding energy, but not peak c . However, this calculated peak was found to have the wrong polarization dependence to be the experimental peak b , instead show-

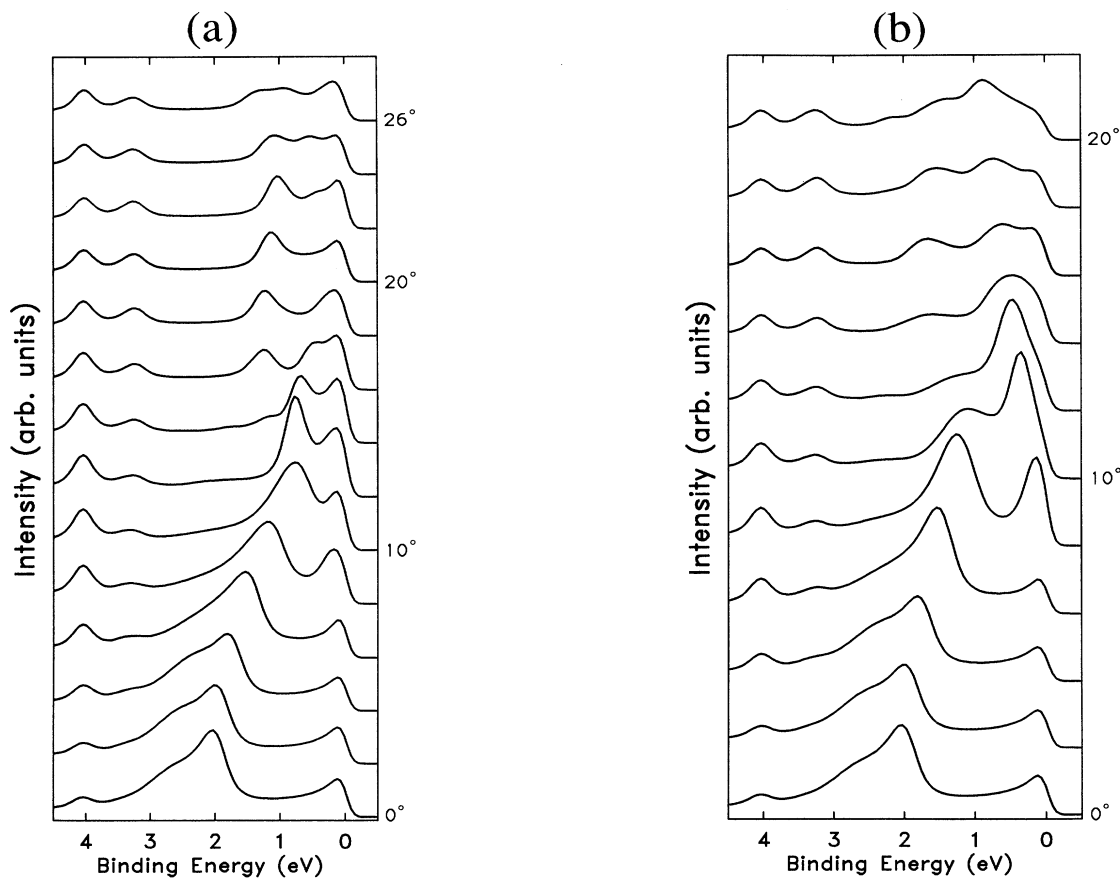


FIG. 12. Calculated off-normal-emission ARUPS spectra, photon energy 40 eV, p -polarized, incident at 55° , with emission angles varying along (a) ΓKM and (b) ΓM .

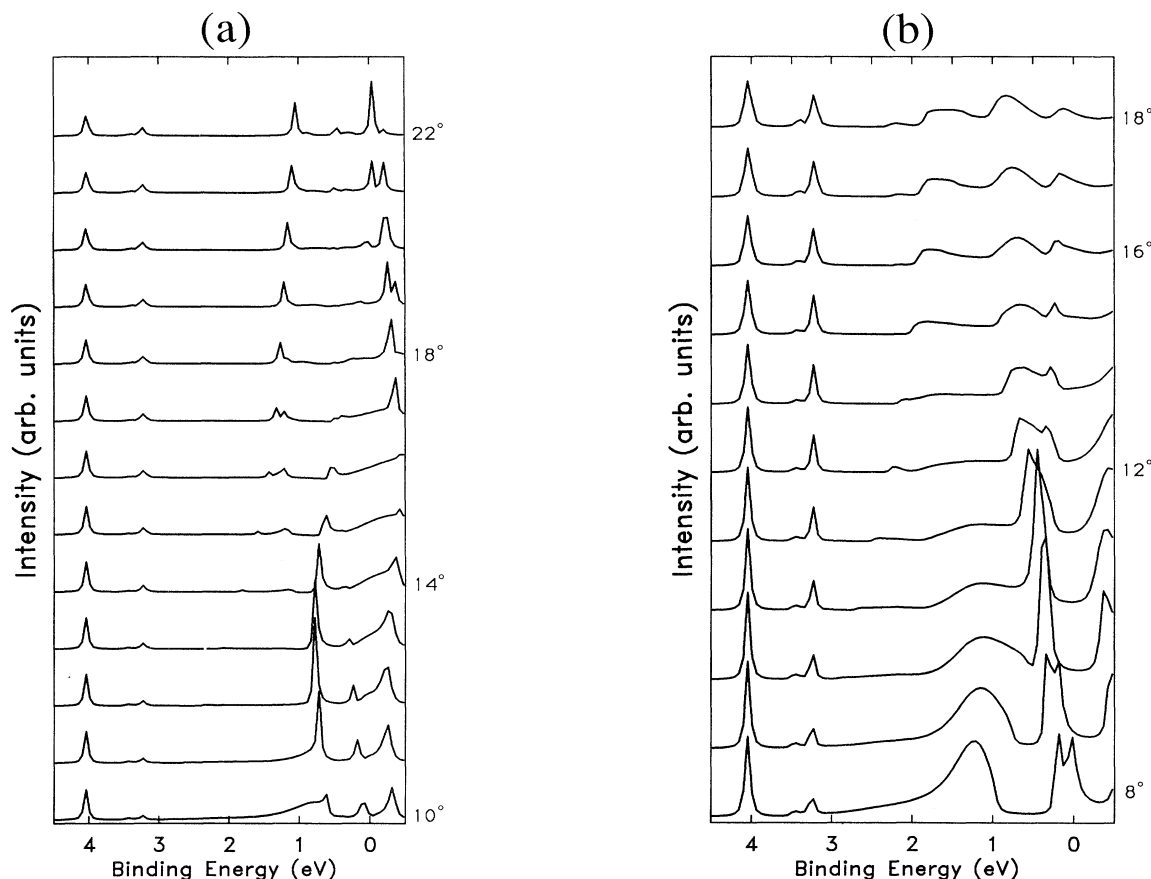


FIG. 13. Calculated ARUPS spectra, with emission angles along (a) ΓKM and (b) ΓM , with the same photon parameters as those of Fig. 10, but with the inverse lifetime of the initial-state hole reduced to an artificially low value. These spectra have not been truncated or convoluted.

ing the same dependence as peak *c*. Further, the photon energy dependence of the calculated peak is very similar to that of peak *c* (Fig. 11) suggesting that the calculated peak at 2.05 eV binding energy in fact corresponds to peak *c*, with the binding energy underestimated by the calculations. Since peaks *a* and *c* were not reproduced in the *Y* calculations,¹² and given the similarity in the calculated band structures of the two elements, this suggests that both these features are due to surface effects.

Figure 12 shows calculated off-normal photoemission spectra, using the same photon energy and incidence angle as was used in the experiment, with emission angles varied along ΓKM and ΓM . In both cases the angles covered correspond to values of k_{\parallel} from zero to the boundary of the first Brillouin zone. Note that although the binding energy of peak *c* is underestimated the extent of its dispersion is correctly calculated. This causes the calculated peak to overlap with the features close to the Fermi level, which obscures the possible Fermi level crossings seen in the experimental data. In order to clarify the detail we repeated the calculations for the regions of interest in smaller angular increments, with the initial-state inverse lifetime decreased. This will reduce the width of the photocurrent peaks without shifting

their position. The results are shown in Fig. 13. For the ΓM direction [Fig. 13(b)] a band does seem to cross the Fermi level at about $\theta=8^{\circ}$, remaining close to the zone boundary. This seems to be in agreement with Fig. 7(b), although the high intensity of peak *a* close to the *M* point, which is not reproduced by the calculations, makes the experimental data unclear. If the band crossing the Fermi level is a bulk band, which is likely given that a such a crossing exists in the bands of Figs. 2 and 3 along ΓM , it is entirely feasible that its intensity relative to peak *a*, which appears to be a surface feature, would be overestimated by the calculation. For the ΓK direction [Fig. 13(a)] there is no obvious crossing, but a feature emerges at $\theta=16^{\circ}$ at ~ 1 eV below the Fermi level. Comparison with Fig. 7(a) suggests that this feature may in fact be responsible for the apparent crossing.

V. CONCLUSIONS

All the features seen in the ARUPS spectra appear to be explicable in terms of emission from one-electron bands; by analogy with the *Y*(0001) results of Barrett and Jordan¹² peak *b* is due to emission from the Γ_{4-} point of

the bulk band structure, and peaks *a* and *c*, and the 4-eV shoulder are reproduced in the photocurrent calculations, which suggest that they are due to surface effects. Since these features are very similar to those seen on Y(0001) (Ref. 12) it follows that the same may also apply to that surface. This supports the suggestions of Barrett and Jordan¹² regarding peak *a*, but contradicts their suggestion that peak *c* is due to a many-body effect. Further ARUPS work on Y(0001) is needed, specifically off-normal-emission measurements to map the surface bands for comparison with those of Fig. 7, before a more definite conclusion regarding the origin of the features on that surface can be reached. The data of Figs. 6 and 7 represent the only detailed surface band mapping of any hcp rare earth yet performed. The wealth of detail present in these data suggests that even subtle trends in electronic structure across the series may well be observable if these experiments are repeated on other hcp lanthanides.

NEWPOOL does not include any relativistic effects, but comparison of the relativistic bands (Fig. 2) with the non-relativistic bands (Fig. 3) shows that the relativistic effects on the electronic structure are insufficient to account for the discrepancy between the observed and calculated binding energies of peak *c*. It is possible that the difference in electron-photon matrix elements between nonrelativistic and relativistic photocurrent calculations could account for the discrepancy but until we are able to perform relativistic photocurrent calculations for this system we are not able to determine this. The differences in binding energies obtained when comparing the theoret-

ical spectra with those of experiment may well be due to the inadequacies of the model. While the use of slab potentials represents a significant improvement over the rather crude NEWPOOL surface model (Fig. 8), the surface potential remains somewhat inaccurate; we cannot calculate the work function or the surface energetics, for example. Another possibility is that self-energy effects, which the code does not take into account, play an important role in the photoemission process. In principle self-energy effects could be included within the NEWPOOL code,³⁰ but the presence of localized 4*f* levels both above and below the Fermi level means that it is unlikely that meaningful calculations of the self-energy for Ho can be performed. However, even at the present level of sophistication the photocurrent calculations have proven to be invaluable in the interpretation of ARUPS results from rare-earth metals.

ACKNOWLEDGMENTS

We would like to thank Dr. David Fort for supplying the high-quality holmium crystal. The assistance of Dr. Tracy Turner, and the rest of the support staff at the SRS, is gratefully acknowledged. N.H. acknowledges the University of Liverpool for financial support. R.I.R.B., S.S.D., and A.M.B. acknowledge the provision of SERC support, and A.M.B. also acknowledges the additional support of the Department of Physics, Florida Atlantic University. This work was funded by SERC and the European Community.

- ¹*Valence Instabilities and Related Narrow Band Phenomena*, edited by R. D. Parks (Plenum, New York, 1977).
- ²G. Rossi, Surf. Sci. Rep. 7, 1 (1987); L. Duo, M. Sancrotti, R. Cosso, S. D'Addato, A. Ruocco, S. Nannarone, D. Norman, and P. Weightman, Phys. Rev. B **42**, 3478 (1990), and references therein.
- ³S. D. Barrett, R. I. R. Blyth, A. M. Begley, S. S. Dhesi, and R. G. Jordan, Phys. Rev. B **43**, 4573 (1991).
- ⁴S. H. Lui, in *Handbook of Physics and Chemistry of Rare Earths*, edited by K. A. Gschneidner and L. Eyring (North-Holland, Amsterdam, 1978), Vol. 1, p. 233; B. N. Harmon, J. Phys. (Paris) Colloq. **40**, C5-5 (1979), and references therein.
- ⁵N. V. Smith, in *Photoemission from Solids I: General Principles*, edited by M. Cardona and L. Ley (Springer-Verlag, Berlin, 1978), p. 237.
- ⁶B. J. Beaudry and K. A. Gschneidner, in *Handbook of Physics and Chemistry of Rare Earths*, edited by K. A. Gschneidner and L. Eyring (North-Holland, Amsterdam, 1978), Vol. 1, p. 73.
- ⁷F. J. Himpsel and B. Reihl, Phys. Rev. B **28**, 574 (1983).
- ⁸J. O. Dimmock and A. J. Freeman, Phys. Rev. Lett. **13**, 750 (1964).
- ⁹W. M. Temmerman and P. A. Sterne, J. Phys. Condens. Matter **2**, 5529 (1990).
- ¹⁰D. Weller, S. F. Alvarado, W. Gudat, K. Schroder, and M. Campagna, Phys. Rev. Lett. **54**, 1555 (1985).
- ¹¹S. C. Wu, H. Li, D. Tian, J. Quinn, Y. S. Li, F. Jona, J. Sokolov, and N. E. Christensen, Phys. Rev. B **41**, 11 911 (1990).
- ¹²S. D. Barrett and R. G. Jordan, Z. Phys. B **66**, 375 (1987).
- ¹³S. D. Barrett, A. M. Begley, and R. G. Jordan, J. Phys. F **17**,

- L145 (1987).
- ¹⁴S. D. Barrett, R. I. R. Blyth, S. S. Dhesi, and K. Newstead, J. Phys. Condens. Matter **3**, 1953 (1991).
- ¹⁵E. Jensen and D. M. Wieliczka, Phys. Rev. B **30**, 7340 (1984).
- ¹⁶G. Rosina, E. Bertel, F. P. Netzer, and J. Redinger, Phys. Rev. B **33**, 2364 (1986).
- ¹⁷J. K. Lang, Y. Baer, and P. A. Cox, J. Phys. F **11**, 121 (1981); F. Gerken, A. S. Flodstrom, J. Barth, L. I. Johnson, and C. Kunz, Phys. Scr. **32**, 43 (1985).
- ¹⁸H. L. Skriver, *The LMTO Method* (Springer-Verlag, Berlin, 1984).
- ¹⁹U. von Barth and L. Hedin, J. Phys. C **5**, 1629 (1972).
- ²⁰D. D. Koelling and B. N. Harmon, J. Phys. C **10**, 3107 (1977).
- ²¹K. N. R. Taylor and M. I. Darby, *Physics of Rare Earth Solids* (Chapman and Hall, London, 1972).
- ²²P. Blaha, K. Schwarz, and P. H. Dederichs, Phys. Rev. B **38**, 9368 (1988).
- ²³A. M. Begley, Ph.D. thesis, University of Birmingham, 1990.
- ²⁴R. I. R. Blyth, R. Cosso, S. S. Dhesi, K. Newstead, A. M. Begley, R. G. Jordan, and S. D. Barrett, Surf. Sci. **251/252**, 722 (1991).
- ²⁵R. G. Jordan, Phys. Scr. **T13**, 22 (1986).
- ²⁶C. G. Larsson, Surf. Sci. **152/153**, 213 (1985).
- ²⁷S. Tougaard and A. Ignatiev, Surf. Sci. **155**, 270 (1982).
- ²⁸R. G. Jordan, A. M. Begley, S. D. Barrett, P. J. Durham, and W. M. Temmerman, Solid State Commun. **76**, 579 (1990).
- ²⁹R. I. R. Blyth, P. T. Andrews, and S. D. Barrett, J. Phys. Condens. Matter **3**, 2827 (1991).
- ³⁰R. G. Jordan, J. Phys. Condens. Matter **1**, 9795 (1989).